Mon. Not. R. Astron. Soc. **296,** 33–43 (1998)

X-ray binary unified analysis: pulse/RV application to Vela X1: GP Velorum

R. E. Wilson and D. Terrell
Astronomy Department, University of Florida, Gainesville, FL 32611, USA

Accepted 1997 October 10. Received 1997 July 14

ABSTRACT

A procedure for simultaneous analysis of multiple kinds of observations is developed for binaries that contain X-ray pulsars. A wide variety of observation types might be included, although we consider only velocity: pulse and light: velocity: pulse cases at present. The model operates with equipotentials and can accommodate non-synchronous rotation and eccentric orbits. The duration condition imposed by observed X-ray eclipses is incorporated as an embedded constraint, so that only solutions consistent with the eclipse duration are found. Relations needed for the method of differential corrections in least-squares solutions are specified, and we apply the Marquardt scheme for improvement of solution convergence. Parameters of Vela X1: GP Velorum are obtained from seven combinations of pulse and radial velocity data. The estimated masses are thereby put into some perspective, especially for the neutron star. The mass of the supergiant ($m \sin^3 i$) now ranges only ± 5 per cent from the mean of seven results, although the uncertainty in i makes the actual mass range larger. We discuss the determinacy of certain parameters and their historical consistency. For example, the systemic radial velocity differs among spectroscopic data sets by more than 20 km s^{-1}. We show that, contrary to published assertions, the orbital inclinations of high-mass X-ray binaries are essentially indeterminable by the usual methods, although lower limits to inclination may be meaningful for some examples.

Key words: techniques: radial velocities – binaries: close – binaries: spectroscopic – stars: neutron – pulsars: general.

1 INTRODUCTION

The X-ray binaries are rare but intensively observed objects the many aspects of which have been reviewed by Bahcall (1978), Joss & Rappaport (1984), Nagase (1989) and others. Some X-ray binaries have abundant backlogs of multiple kinds and epochs of observations including radial velocity and light curves, polarimetry, pulse arrival times, and other types. Despite their abundance, the observations often have given mixed messages. Some parts of the problem are related to transient effects and are fundamentally difficult, while others are due to timewise variation of system parameters for which some very effective schemes already exist, such as in the case of variable pulse periods (Nagase et al. 1984). A third category of problem can be traced to non-unified, less than optimal treatment of the various kinds of data sets. These latter problems can be surmounted by properly thought out procedures, with some progress already having been made. Here we extend certain ideas of binary star modelling and analysis to X-ray binary applications, with the supergiant X-ray system Vela X1: GP Velorum (= HD 77581 = 4U 0900−40) as our initial example. We shall refer to the binary as Vela X1 when the context is the neutron star component, and as GP Velorum when it is the B supergiant component. The binary is an example of the class of high-mass X-ray binaries (HMXBs). Our primary objective is to reduce uncertainties arising from problems of analysis and from the combining of multiple types of analytical results, so that remaining uncertainties essentially are due only to the data sets. An idea that has been around for some time (Wilson & Wilson 1976; Wilson 1979) but seldom applied is the use of an observed X-ray eclipse duration not merely as a final filter on solutions, but *as an embedded solution constraint*. An idea with frequent application is that of *simultaneous* least-squares solution of two or more distinct kinds of observations. For example, Wilson & Devinney (1972) solved multi-band light curves simultaneously, Morbey (1975) and Pourbaix (1998) combined radial velocity and visual binary data, and Wilson (1979) combined radial velocities and multi-band light curves. In a conceptually similar development, Nagase et al. (1984) combined multiple epochs of X-ray pulse data. Although not different *kinds* of observations, the multiple X-ray epochs were treated mathematically as distinct data sets, solved simultaneously. Of these combinations, the one that has been most extensively followed up on is the radial velocity: multi-band light curve (e.g. Van Hamme & Wilson 1984, 1986, 1990). The radial velocity: visual binary area is likely to become very important owing to

expected advances in interferometry. Separate analysis of X-ray pulse observations has been an active arena with a number of approaches tried. Although much innovation has been applied to velocity solutions and also to pulse solutions, our contributions are in different areas from those already explored, specifically in several advantageous analytic features that have not previously been used together (see Wilson & Terrell 1994 for a preliminary report).

We combine into one unified procedure (1) an equipotential model for the figure of the optical companion with non-synchronous rotation and eccentric orbit effects (such as proximity effects on radial velocities), (2) an embedded X-ray eclipse duration constraint, (3) simultaneous multi-data fitting, (4) formulation of the method of *differential corrections* specifically for pulse arrival times, with analytic derivatives, and (5) the Marquardt (1963) scheme to improve solution convergence. In regard to lobe filling, we use a generalized definition of the traditional Roche lobe that applies for non-synchronous as well as synchronous rotation and for eccentric as well as circular orbits (Wilson 1979): a limiting lobe is an equipotential (or its contained volume) for which effective gravity is zero on the line of centres at periastron. The solution procedure does not need the intermediate fitting functions and series expansions that one sees in some X-ray pulse papers. We compute only equilibrium rather than dynamical tides, so dynamical tides remain as an unrealized advance in this kind of application. The main dynamical tide effects may only be stochastic variations about equilibrium, although the number of data needed for good averaging may be very large for GP Vel. Still, given the advantages combined here, fitting of X-ray binary data by the least-squares criterion becomes more powerful, more straightforward to apply and to program, and readily amenable to refinements. An example of a further refinement might be added solution parameters such as time derivatives of some of the basic parameters, which would require only additional terms in the least-squares equation of condition.

One might ask if a rigorously unified model and solution are genuinely preferable to existing practice, in which at best one of the above-listed items is used alone. Consider how the geometry and physics of the situation are coupled. Even in the simple case of an equilibrium tide, the surface configuration of the optical star depends on the mass ratio, rotation, orbital eccentricity and instantaneous separation (equivalently, phase). Its projected horizon (relevant to eclipses) depends on all those things plus the argument of periastron and orbital inclination. In this rather complicated situation one sees published parameter estimates via spherical star approximations and a chain of corrections, even in very good review papers. Can such approximations and corrections do as well as a unified treatment? Considering that the approximate way begins with an 'effective mean radius' that has no consistent definition (effective in what sense?), that the chain of corrections is long, and that some corrections are ignored, we think that the answer is 'no'. Even if the answer were as good as 'perhaps', there would be no reason to settle for corrected spherical calculations when a fast computer can provide a full and coherent calculation (Wilson 1979). In addition to the geometrical–physical problem, one has a correlation problem among parameters derived from the various kinds of observations, in that their correlations will be different for optical velocities *vis-à-vis* pulse data *vis-à-vis* light curves, etc. A simultaneous solution can accomodate all the correlations and come to properly adjusted results because it can '*see*' the various influences together, whereas separate pulse, velocity, etc., solutions see only part of the picture. Accurate results via self-consistent analyses are particularly important here because GP Vel is very close to filling its limiting lobe. As we shall see, its delicate lobe filling status is hard to evaluate even with fully consistent X-ray and optical parameters, and even small inconsistencies make evaluation much harder. Naturally, the lobe configuration has major astrophysical significance for present structure and for past and future evolution as well.

Some of the parameters of Vela X1: GP Vel are reasonably well known as a result of numerous observational and analytical papers over the past three decades. However, the masses are very important and their realistic uncertainties are not so well known, as the results depend on which observations are used – especially on the optical velocities – and on how pulse and velocity information is combined. The mass of the X-ray source is especially important for Vela X1 and other X-ray binaries. Relatively high estimates can be interesting with regard to the mass limit for neutron stars. Any estimate is interesting with regard to pre-collapse core masses in the end states of evolution and to the collapse itself. A consensus of published mass estimates indicates that Vela X1 is about 25 per cent more massive than a typical X-ray pulsar, yet one recent estimate (Stickland, Lloyd & Radziun-Woodham 1997) assigns a mass similar to those of other pulsars. Thus one of our main results is a perspective view of Vela X1: GP Vel mass estimates. We make progress by combining the above-mentioned five items that, taken together, increase coherence while decreasing complexity. The explanation in the Appendix should make the procedure easy to program. However this is only a step. Further progress will be needed through generalization of the basics and through continued observations. Indeed, a primary virtue of the procedure lies in its being easy to generalize, largely because Fourier series, polynomial fitting functions and series expansions play no role.

2 SOLUTION STRATEGIES FOR PULSED ECLIPSING X-RAY BINARIES

Our solution strategies differ in several ways from some others, including the independent variable for the pulse analysis. Early work, and now also our work, fits *pulse arrival time* with *pulse number* as the independent variable (e.g. Rappaport, Joss & Stothers 1980; Nagase et al. 1982, 1984; Nagase 1989), while a recent trend has been to fit *pulse delay*, with *time* as the independent variable (van der Klis & Bonnet-Bidaud 1984, hereafter KB; Boynton et al. 1986, BDLZ; Deeter et al. 1987, DBSHNS). We have gone back to the original way because it keeps the overall logic simple and straightforward. While the two approaches may seem equivalent, notice that a certain awkwardness attends pulse delay, treated as the dependent variable. Scientific tradition is to compare observation as directly as possible with theory, as in comparing observed and theoretical pulse arrival times. While pulse delay is a computable theoretical quantity (it is just a light traveltime in the model), it has no purely observational counterpart. An 'observed' pulse delay is the difference between *arrival time* and *expected arrival time in the absence of an orbital light time effect*. (Negative delays will still be called delays, not 'advances'.) Although *arrival time* is a direct observable, *expected arrival time* depends on various model parameters (how large is the orbit, when was the nodal crossing of the star, etc.) so that pulse delay is an observational–theoretical hybrid. As a consequence, 'observed' delays are not definite until the parameters have been adjusted (one has to know the answers to get the answers). The authors who fit pulse delays rather than arrival times utilize Fourier or other fitting functions, coupled to series expansions, to deal with this problem.

While that method can be effective and accurate, lack of need for intermediate fitting functions and series expansions makes the original one more straightforward and therefore more readily extendable. It can be applied because, for many real data sets, we do presume to know the integer pulse numbers, reckoned from some reference pulse, and the pulse numbers are just the integer part of a more general *pulse phase*. We thus adopt the pulsar as a fundamental clock and conceptually plot arrival time (including delays) against pulsar phase (no delays). We would like the pulsar clock to be steady in the interest of accurate results, but must realize that its short-term variations are intrinsic to the problem and degrade accuracy no matter how the analysis is done. Although the strategy will fail if the pulsar clock is so unsteady that one cannot identify correct pulse numbers, the same failure will attend other methods.

One can still graph *pulse delay* for illustrative purposes because, after a solution is completed, we have numbers for the parameters, so *expected arrival time* can be computed without introducing an extra level of iteration or series expansion. Delays really are needed for illustration because the data actually analysed, pulse arrival time versus pulse phase, will look quite straight in a graph – the eye will not see the tiny periodic displacements. Of course, this subjective problem does not bother the least-squares algorithm in the slightest, so we do the actual fitting in arrival times and the illustrations in delays.

3 MULTI-DATA ANALYSIS AND SIMULTANEOUS SOLUTION

Our procedure is direct. We write the pulse arrival time in Heliocentric Julian Date, t, as

$$t = t_{\rm ref} + S(n - n_{\rm ref})P_{\rm p} + \Delta t - \Delta t_{\rm ref}, \tag{1}$$

with $t_{\rm ref}$ the arrival time of a reference pulse (which defines pulse phase zero) and Δt and $\Delta t_{\rm ref}$ the light time delays for a given pulse and the reference pulse, respectively. Apart from notation the basic relation is the same as in Nagase et al. (1984). A superficial distinction is that (1) explicitly contains the separate pulse numbers and separate delays (light travel times) for an arbitrary pulse and the reference pulse, whereas Nagase et al. write pulse numbers and delays already as differences from the reference values. The binary system parameters are contained in the delay terms, the form of which is given in detail in the Appendix. In the pulsar clock term, $n - n_{\rm ref}$ is the number of pulses before or since the reference pulse, with $P_{\rm p}$ the pulse period in seconds, and S a units conversion factor that here is the number of mean solar days in a second of time. Natural refinements could include additional terms for time derivatives of $P_{\rm p}$ (Nagase et al. 1984 already include these) and a relativistic treatment, but for now we keep the exposition simple, as our main thrust concerns items (1) to (5) of the Introduction. Now simply differentiate equation (1) to provide coefficients for a least-squares solution by the method of *differential corrections*, whose equation of condition is

$$t_{\rm o} - t_{\rm c} = \frac{\partial t_{\rm c}}{\partial t_{\rm ref}}\delta t_{\rm ref} + \frac{\partial t_{\rm c}}{\partial P_{\rm p}}\delta P_{\rm p} + \text{binary system terms}. \tag{2}$$

Here $t_{\rm o} - t_{\rm c}$ is the difference between observed and computed pulse arrival times, and $\delta t_{\rm ref}$, $\delta P_{\rm p}$, etc., are corrections to initial parameter estimates. Complete formulations for the partial derivatives are given in the Appendix for parameters i(orbital inclination), $a = a_1 + a_2$(relative orbital semi-major axis), e(orbital eccentricity), ω(argument of periastron), $t_{\rm ref}$, $P_{\rm p}$, t_0 (time of reference orbital conjunction), $P_{\rm orb}$(orbital period) and q (mass ratio $= m_2/m_1$). Equation (1) is the key element. If others prefer not to program the partial derivatives in equation (2) analytically, the derivatives can be evaluated with adequate accuracy by differencing, although direct evaluation by the expressions in the Appendix is probably easier. If terms involving second derivatives are added, one again has the option of forming them analytically or by differencing. Although numerical second derivatives can be awkward to program in some circumstances, here we have analytic first derivatives, which make the differencing simple to program. Accuracy should seldom be a problem, so the choice of method is mainly a matter of programming preference. In this paper we use the basic form (2) for the pulse arrival part of *differential corrections*, programmed with analytic derivatives.

The light curve and radial velocity (hereafter RV) curve parts of the problem are the same as in Wilson (1979), where our overall scheme for carrying out simultaneous differential corrections solutions in parameters $p_1, p_2, \ldots\ldots, p_n$ is explained in some detail. Equation (19) of that paper (here with slight notation changes),

$$f_{\rm o} - f_{\rm c} = \frac{\partial f_{\rm c}}{\partial p_1}\delta p_1 + \frac{\partial f_{\rm c}}{\partial p_2}\delta p_2 + \ldots\ldots + \frac{\partial f_{\rm c}}{\partial p_n}\delta p_n, \tag{3}$$

utilizes the general symbol f to represent light, RV, pulse arrival time, or any other kind of observation. Although time is the natural independent variable in light curve and RV curve solutions, there is no need for the several parts of a simultaneous *differential corrections* solution to have the same independent variable. In the present case of light: velocity: pulse or velocity: pulse solutions, time remains a natural independent variable for the light and RV parts while pulse phase is natural for the pulse part. We therefore adopt (3) as our general least-squares equation of condition, with the understanding that f means light or RV or pulse arrival time as the case may be for particular observations. Thus the $t_{\rm c}$ of (2) (specific equation for pulses) becomes $f_{\rm c}$ when used in (3).

Computation of the surface configuration at arbitrary phase and thus also the mean radius for the eccentric, non-synchronous case are covered in Wilson (1979). Although numerous papers have used X-ray eclipse duration to limit parameter ranges, only Wilson & Wilson (1976) have applied it as an embedded constraint, and then only in the special case of synchronous rotation and circular orbit for light curve solutions. An unconstrained least-squares solution (adjusting mean radius among the other parameters) will violate the duration condition in most examples because light and RV curves of HMXBs provide only weak information on the size and figure of the optical star. Of course one can simply step the mean radius (or periastron potential) and find a family of solutions consistent with the range of observed durations. However, one would first have to guess a range of mean radii and proceed by trial and error. To find a solution for a definite eclipse duration (say the longest, shortest or average observed) one must then either go through an extra level of iteration or interpolate all system parameters and their standard errors from tables of solutions. These difficulties are eliminated by embedding the eclipse duration constraint within the procedure.

Convergence is greatly improved by application of the well-known Marquardt (1963) scheme, and we find that Marquardt λs in the range 10^{-4} to 10^{-7} give essentially the same (good) convergence behaviour. One also might try solutions via algorithms other than *differential corrections*, perhaps one such as Simplex that requires no derivatives. In that case equation (1) or an extension with more parameters provides the entire modelling formalism. We prefer *differential corrections* because it is fast and, more importantly, because it allows one to change the parameter set under adjustment very easily at any point in the iterations. With inclusion of the Marquardt λ, it usually converges extremely well.

Discussions of the relative merits of various solution algorithms that might be used with equation (1) can be found in many places, such as Barone et al. (1988), Price (1976), Kallrath & Linnell (1987), Plewa (1988), Wilson (1994), and the references contained in those papers.

4 VELA X1: GP VEL SOLUTIONS

Our original intent was to fit light, radial velocity and pulse curves simultaneously. However, the light curves of GP Vel are seriously affected by dynamical and essentially stochastic (probably tidal) disturbances (Tjemkes, Zuiderwijk & van Paradijs 1986; Wilson & Terrell 1994; van Kerkwijk et al. 1995). It seems unlikely that the mechanisms of these disturbances can be modelled realistically in the near future. Ours is a physical model in that it incorporates gravitational–centrifugal equipotentials and their timewise variation [Wilson (1979); see also Tjemkes et al. (1986) for a similar model; see Plavec (1958) and Limber (1963) for the non-synchronous potential, and Avni (1976) for the eccentric potential] but it is not a structural–hydrodynamical model, nor does an adequate such model now exist. Within the large scatter, our computed light curves and those of Tjemkes et al. (1986) show good agreement with those of GP Vel in regard to waveform, which is distinctly different from a pure sinusoid. However, the computations have only about half the observed amplitude and a phase shift of 0.04 cycle. The waveform and the amplitude mismatch are nicely shown by fig. 12 of Tjemkes et al. (1986), while fig. 1 of Wilson & Terrell (1994) shows those features and also the 0.04-cycle phase shift. Put simply, present models are not adequate to deal with the complicated dynamical tides in GP Vel in regard either to light curve amplitude or to phase lag. However, our model does have a phase-variable equilibrium tide, which in itself is a major asset for computation of light curves and to some extent also for RV curves. Sterne (1941), Hutchings (1973), Wilson & Sofia (1976), van Paradijs, Takens & Zuiderwijk (1977a), Wilson (1979) and Van Hamme & Wilson (1994, 1997) discuss and compute such RV distortions.

There are good U, B, V, L, W light curves (Walraven system) by van Genderen (1981) that contain important information, and we initially included them in simultaneous light: velocity: pulse solutions. The van Genderen light curves are the best set for GP Vel in regard to wavelength and phase coverage and for internal coherence, although many other light curves and fragments of light curves exist. Subjective fits to mean light curves were discussed in considerable detail by Tjemkes et al. (1986), using a figure computation scheme substantially identical to that in Wilson (1979). They did not try to adjust q but adopted a fixed value of 12.8, which approximately corresponds to the relative pulse and optical velocity amplitudes, although somewhat lower than recent estimates. They found, as did Wilson & Terrell (1994), that the observed amplitude of ellipsoidal variation is much larger than one expects from an equilibrium tide. Not surprisingly, when we adjusted q in our light: velocity: pulse solutions, it ran to obviously wrong (low) values as the model tried to mimic the large ellipsoidal variation in the many light curve points. This outcome can be viewed as a success rather than a failure because it sends a clear message that the tide is not an equilibrium tide.

Although our procedure applies to simultaneous light: velocity: pulse data and we have carried out a few such solutions, we report only simultaneous velocity: pulse solutions for the reasons already mentioned, connected with light curve problems. Other decisions also must be made before solutions can properly be carried out. The adjusted parameters should be those that influence the RV and/or pulse observations to a reasonable degree and are not hopelessly correlated with other parameters. Periastron potential, Ω_2, is computed as $\Omega_2(q, e, \omega, F_2, i, \Theta_e)$ according to the rules in Wilson (1979) and therefore is not adjustable. Parameter F_2 is the ratio of the angular rotation rate of the optical star to the mean orbital rate, and Θ_e is half the phase duration of X-ray eclipse. Here we adjust a, e, ω, V_γ, t_{ref}, P_p and q. The binary system centre-of-mass velocity, V_γ, effectively relates only to RVs and not to pulses, as it is perfectly correlated with P_p for pulse-only data sets. Any ω listed or discussed here is ω for the X-ray source (star 1), not for the optical star (which would differ by 180°). The binary system parameters a, e, ω and q reflect the influences of both RV and pulse observations, balanced in the simultaneous solutions according to the assigned weights. The ratio of RV to pulse weights is the inverse ratio of the data variances, with the variances determined from the residuals as part of the iterative solutions. All weights are the same within any

Table 1. Θ_e versus F_2 and i for seven solutions.

Sol.	F_2	Ω_{lobe}	$i = 90°$	$i = 85°$	$i = 80°$	$i = 75°$	$i = 70°$
1	0.0	17.8506	.0996	.0990	.0971	.0937	
	0.5	18.8541	.0982	.0975	.0954	.0918	
	1.0	21.7324	.0938	.0930			
2	0.0	18.8071	.0951	.0944	.0925		
	0.5	19.7599	.0911				
3		lobe	exceeded				
4	0.0	17.5313	.1009	.1002	.0983	.0949	.0898
	0.5	18.5368	.0994	.0987	.0966	.0929	
	1.0	21.4175	.0949	.0940	.0913		
5	0.0	16.9858	.1021	.1014	.0995	.0961	.0910
	0.5	17.9855	.1005	.0998	.0977	.0940	
	1.0	20.8446	.0958	.0949	.0922		
6	0.0	17.6895	.0973	.0967	.0949	.0916	
	0.5	18.6493	.0960	.0953	.0933		
	1.0	21.4051	.0918	.0910			
7	0.0	19.6530	.1015	.1009	.0991	.0959	.0911
	0.5	20.8161	.1000	.0994	.0974	.0939	
	1.0	24.1536	.0955	.0947	.0921		

Table 2. Adjusted parameters and standard deviations from seven solutions.

Solution/ Source	$a \sin i$ ($R_\odot$)	e	ω (°)	$T_0 - 2444612.$ (*Hel.JD*)	$T_0 - 2443819.$ (*Hel.JD*)	$T_0 - 2442612.$ (*Hel.JD*)	V_γ ($km\,s^{-1}$)	$P_p - 282.$ (*s*)	m_2/m_1
1	52.94	.0917	137.9		.9781793		−8.42	.74961	14.53
A,b	±.50	±.0078	±6.4		±.0000080		±.82	±.00056	±.93
2	53.74	.1206	146.1			.841432	−8.4	.89595	14.6
A,a	±.80	±.0092	±7.7			±.000015	±1.7	±.00090	±1.9
3	54.6	.127	140			.841443	−5.8	.8963	13.5
B,a	±1.3	±.018	±14.			±.000028	±1.7	±.0017	±1.6
4	54.09	.085	139.4	.306942			+13.7	.85039	14.4
C,c	±.45	±.010	±5.2	±.000011			±1.3	±.00048	±1.3
5	52.52	.075	136	.305950			+13.6	.88400	14.0
C,d	±.84	±.025	±11.	±.000055			±1.3	±.00098	±1.4
6	53.40	.098	132.7		.978175		+13.6	.74984	14.2
C,b	±.64	±.011	±7.7		±.000011		±1.2	±.00074	±1.2
7	52.69	.0923	134.7		.9781770		−3.47	.74980	16.6
D,b	±.53	±.0082	±6.4		±.0000080		±1.02	±.00056	±1.6

A = van Paradijs et al. (1977b) mean of He I lines.
B= Petro & Hiltner (1974) 'mean' plus Wallerstein (1974) 'absorption blue'.
C= van Kerkwijk et al. (1995) (their table 1 plus their table 3).
D = Stickland et al. (1997).
a = july75 (as listed in table 6 of BDLZ).
b = nov78 (as listed in table 6 of BDLZ).
c = jan81, 1st orbit (as listed in table V of DBSHNS).
d = jan81, 2nd orbit (as listed in table V of DBSHNS).

RV or pulse data set. We did not adjust the orbital ephemeris because the pulse data sets typically are shorter than one orbit cycle and most of the RV sets span only small parts of the historical record. Instead we adopted the orbital period, $P_{orb} = 8.964\,43$ d, and the orbital reference epoch, $t_0 = $ JD 244 3821.8604 from BDLZ, which were found from long stretches of data. In both BDLZ and here, t_0 is a time of superior conjunction of the neutron star. There is no chance to find i or F_2 without the help of light curves, so we ran solutions only for $i = 90°$ and $F_2 = 0$ (no rotation), which is the safest case if we want to avoid overfilling of the supergiant's limiting lobe. We verified that solutions with other fixed F_2s lead to the same parameter values, within the standard errors, and that solutions for $i < 90°$ also do so, except of course for parameter a, which always satisfies the relation $a \sin i \approx$ constant.

The role of eclipse semi-duration, Θ_e, is almost entirely to delimit the permitted F_2 and i ranges because pulse arrival times are unaffected by Θ_e and RVs are almost unaffected. Therefore *any* $[F_2, i]$ pair that gives the observationally adopted Θ_e, and does not violate the limiting lobe condition, is valid. So one can change Θ_e without much altering velocity: pulse solutions (but of course not light: velocity: pulse solutions). Thus Θ_e is given as a function of F_2, i for each of our solutions in Table 1. From the table one can estimate the largest F_2 and smallest i allowed for any adopted Θ_e. In principle, Θ_e has some small influence on theoretical RVs because it affects the surface configuration of star 2. It has a major influence on light curves through ellipsoidal variation, but our listed solutions are for velocity: pulse only. Estimates of Θ_e from X-ray observations include 0.106 ± 0.003 by Forman et al. (1973), 0.100 ± 0.002 by Charles et al. (1978), 0.094 ± 0.004 by Watson & Griffiths (1977), 0.106 ± 0.003 by Ogelman et al. (1977), 0.089 ± 0.003 by Nagase et al. (1983) and 0.096 ± 0.003 by Sato et al. (1986). There have been previous attempts to reconcile the rather wide eclipses with a physically consistent geometry in which the supergiant does not exceed its limiting lobe (e.g. Wilson 1979; Tjemkes et al. 1986; van Kerkwijk et al. 1995). Neither the observational nor theoretical Θ_e situations, nor their small range of overlap, seem to be improving. We have adopted Watson & Griffiths' Θ_e because the authors give a thoughtful description of how Θ_e was derived, rather than only mentioning a number, and their procedure seems appropriate. Also, a significantly larger Θ_e makes it very difficult to find solutions that do not violate the lobe-filling condition (i.e. the legitimate F_2, i entries of Table 1 shrink almost to zero ranges). The Nagase et al. (1983) Θ_e is relatively small ('safe') but we decided against using the most extreme value in print. Our results do effectively apply to ranges of Θ_e, not just exactly 0.094, as discussed above. The X-ray eclipse duration constraint for Vela X1: GP Vel may seem to have only limited usefulness here, partly because our listed solutions include no light curves and partly because the observational value of Θ_e is rather uncertain. However, Table 1 defines relations between F_2 and i that essentially apply not only for our adopted Θ_e, but for any Θ_e determined in the future. Since the parameters, given in Table 2, depend only very slightly on Θ_e, the solutions remain realistically valid for any adopted Θ_es that do not lead to overspilling of the lobe. From a parameter estimation viewpoint they remain valid even for modest lobe excesses, although they then become unphysical. With or without light curves, the embedded Θ_e constraint allows one to vary Θ_e in a sequence of solutions while keeping the parameters mutually consistent. A major practical advantage is a saving of printed words, as discussions of how to work back and forth among separated pulse, RV and light curve parts of a solution become unnecessary.

Mass results for the neutron star depend heavily on which optical RVs are processed. Even a quick visual scan shows the amplitude and mean level of RVs to change from one data set to another. Formal error estimates have very limited value in this situation, with systematic effects causing major epoch-to-epoch changes. To illustrate, we find a systemic velocity, V_γ, of $+13.6 \pm 1.3$ s.d. km s^{-1} for one data set and -8.4 ± 1.7 km s^{-1} for another, and one can readily see the reason (a large vertical shift) simply by looking at the

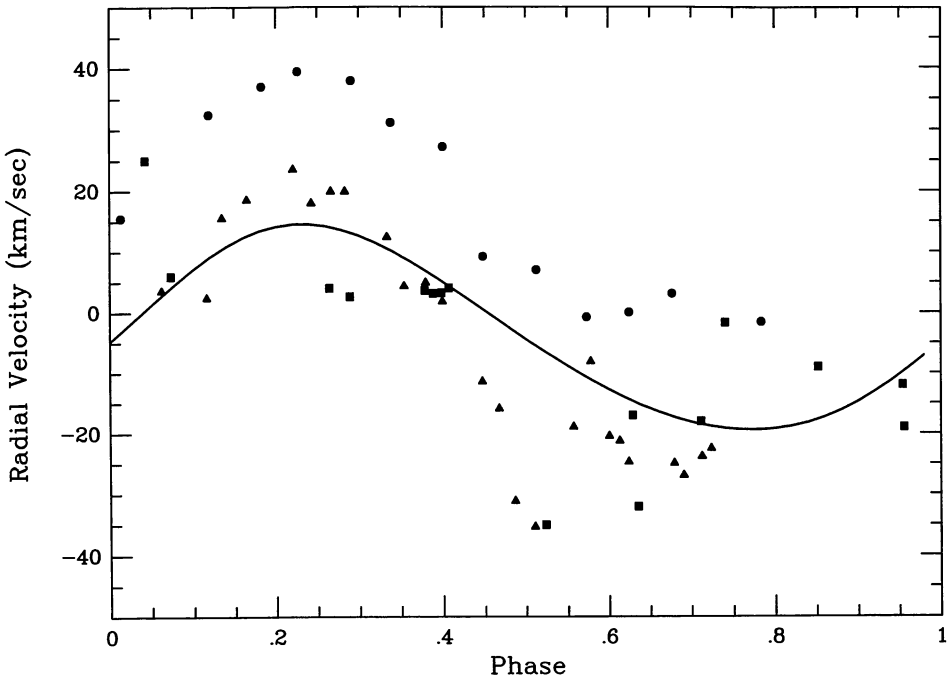

Figure 1. Comparison of the Petro & Hiltner (1974) (squares), Wallerstein (1974) (triangles), and van Kerkwijk et al. (1995) (dots) radial velocities, to illustrate disagreements among data sets. Our solution to a fourth set (Stickland et al. 1997) is shown for reference as the solid curve.

corresponding RV graphs in the original papers. Fig. 1 compares three of the RV data sets and one of our solutions. Fig. 2 shows our fit to the Stickland et al. (1997) RVs, which are the most normal in appearance of published sets.

Amplitude variation is not as large as V_γ variation, but masses are sensitive to RV amplitude, so again epoch-to-epoch changes are important. Given this state of affairs, our response was to do solutions with various combinations of pulse and RV data sets, so as to acquire a feeling for the realistic uncertainties. We thus selected combinations of four RV sets and four pulse sets for simultaneous solution. To this end we examined the distribution of observations over the past 25 years so as to match pulse data with RV data from roughly the same epochs. Previous analyses indicate that the orbital parameters are not changing rapidly with time, with mainly only upper limits on their time derivatives, so mismatches of a few years should not be very important. Nevertheless, we would not want mismatches in the temporal data centroids to be larger than necessary, so we paired RV and pulse sets accordingly, with seven of the 16 possible combinations selected. Time placement and availability (extremely few pulse data are published) were the main considerations in selecting and pairing data sets. A secondary consideration for RVs was night-to-night and cycle-to-cycle consistency. Specifically *not* considered was 'normality' in overall amplitude or V_γ, because one of our main objectives was to acquire a feeling for how parameters jump around owing to systematic differences among data sets. Atypical data sets could give the best information about the underlying binary, since major disturbances may be absent only at a few epochs. The data sets and their pairings are identified by letters A, B, C, D (for RVs) and a, b, c, d (for pulses) in Table 2. Pulse sets c and d are respectively from the first and second orbits of the DBSHNS 1981 January data set. We fitted the two orbits separately because the pulse period was changing unusually rapidly at that time. Constant pulse period was not a good assumption even over as short an interval as two orbits. Fig. 3 is a delay curve for the 1978 November pulse data that shows the smallness of pulse residuals compared with RV residuals.

We have not processed multiple disconnected epochs of pulse data as in several papers by the Nagase group (e.g. Nagase et al. 1984) but expect to do so in the future. The Nagase et al. type of multiple-epoch solution is simultaneous. It might seem not to be so because if one did that for light or RV it would merely be a matter of tossing all observations in together and would not be conceptually different from an ordinary solution. However, the pulse situation is different because it requires knowledge of correct integer pulse numbers and in practice it is seldom possible to know them for even moderately separated epochs. The Nagase group solved this problem by introducing separate reference pulses and separate initial time references for the various epochs of pulse data, and this practice constitutes a true simultaneous solution because those parameters take on different values for different data subsets. We did not solve multiple pulse epochs together because our emphasis is on unified light: velocity: pulse solutions and because most of the relevant pulse arrival times are unpublished. Even if those arrival times were available, significant improvement on the existing analysis (see Nagase 1989 for a review) seems unlikely, as pulse period is a rather robustly determined parameter.

5 SUMMARY AND DISCUSSION

There are many extensive parameter listings and discussions for Vela X1: GP Vel, including their uncertainties and the means by which they were derived. Because undue space would be needed to put all such things in perspective, we make limited comparisons that emphasize differences of primary astrophysical importance, mainly in the mass results. The robust parameters $a_1 \sin i$ and (variable) P_p come from the pulse data and are summarized by Nagase (1989). For comparison with $a_1 \sin i$ in other papers, our $a \sin i = [(1+q)/q]a_1 \sin i$. Our P_p values of Table 2 fit in smoothly with the extensive listing by Nagase (1989).

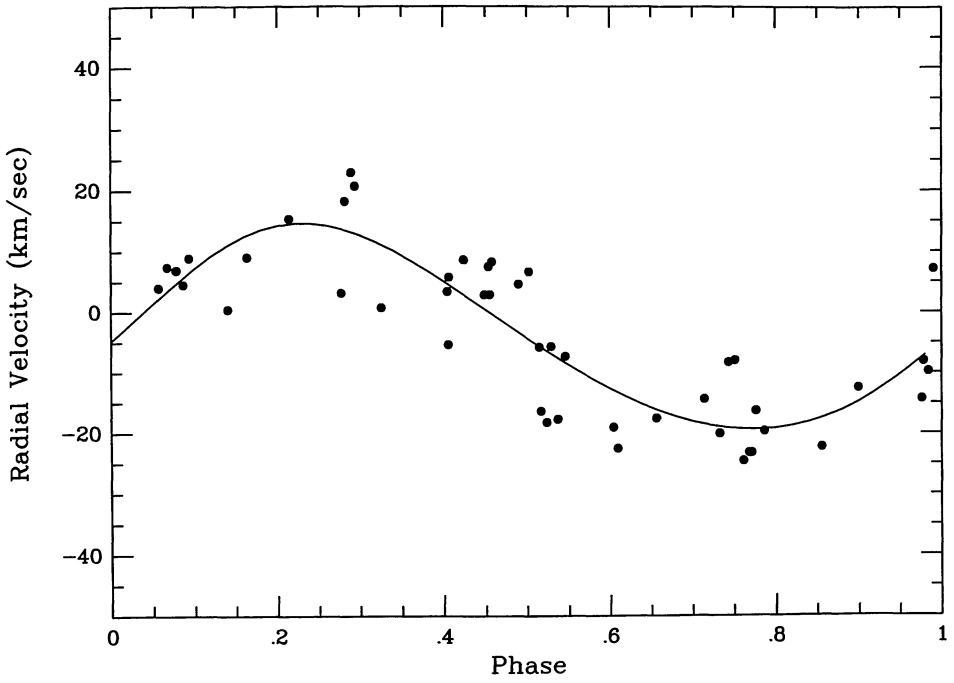

Figure 2. The Stickland et al. (1997) RVs and our solution curve (same curve as in Fig. 1).

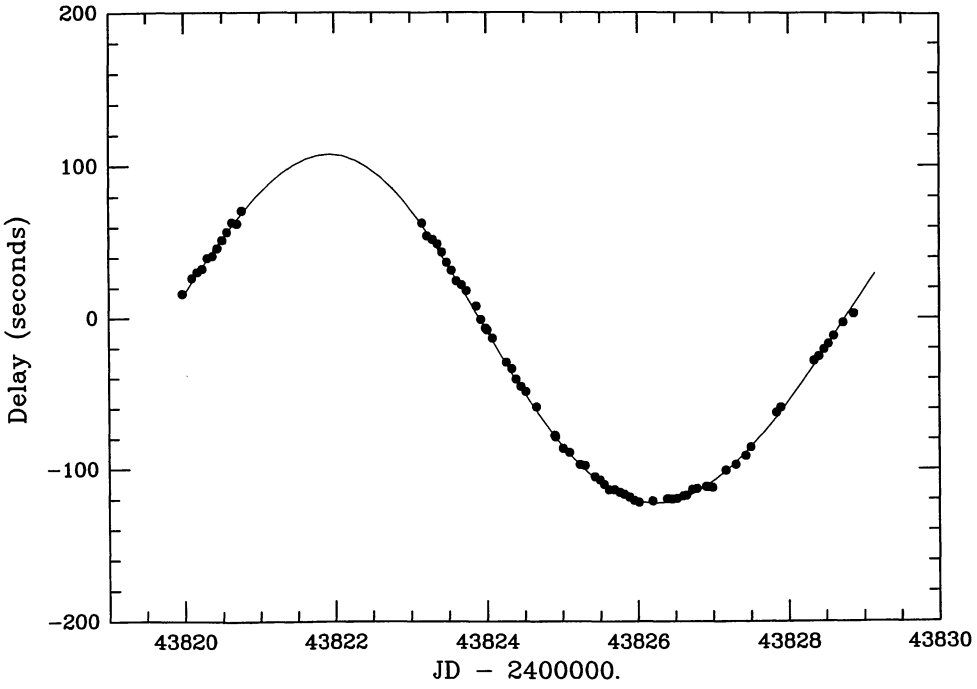

Figure 3. The 1978 November pulse data, referenced in table 6 of BDLZ, and our solution curve.

Other listings from various epochs are in KB, BDLZ and DBSHNS.

The result of main astrophysical significance is the neutron star mass because of implications for its mode of formation. Theoretical and observational estimates of neutron star masses were examined by Timmes, Woosley & Weaver (1996). The collapse-explosions had been followed by Woosley & Weaver (1995). Observational examples included both radio and X-ray binary pulsars. The theoretical distributions are strongly bi-modal, with average masses in the two peaks of 1.28 ± 0.06 and 1.73 ± 0.08 $M_{\odot}$. Those masses do not include accretion from beyond the iron core in the early collapse stages, fallback at late times from material that fails to reach escape speed, or subsequent accretion from the companion, so they are best regarded as lower limits. They also are affected by uncertainties in convection theory. Note that the recent Stickland et al. RVs (both our analyses and Stickland et al.'s) give estimates in

Table 3. Relative radii and related quantities for seven solutions.

Soln.	Ω_2	R_2/a	$R_{\rm lobe}/a$	lobe status	$m_1 \sin^3 i$ $M_\odot$	$m_2 \sin^3 i$ $M_\odot$
1	19.0259	0.5888	0.6186	5% under	1.60	23.26
2	19.0413	0.5939	0.5996	1% under	1.67	24.34
3	17.4009	0.5987	0.5880	2% over	1.88	25.33
4	18.9497	0.5859	0.6221	6% under	1.73	24.39
5	18.6015	0.5842	0.6267	7% under	1.61	22.65
6	18.3762	0.5938	0.6116	3% under	1.68	23.83
7	21.3995	0.5903	0.6296	6% under	1.40	23.12

the lower peak, while a consensus from other published RV curves is in the upper peak (see next paragraph). Obviously the observational range for Vela X1 will have to be narrowed greatly to be useful, since it does not even discriminate between the peaks at present. The variety of estimates depends partly on the observations and partly on how they are analysed, including how the pulse and RV results are combined. Here we analysed representative combinations of pulse and RV data sets, simultaneously and impersonally, and the data sets themselves now appear to be the only significant sources of epoch-to-epoch differences. For each of our solutions, the supergiant's surface 'potential', Ω_2, the mean relative radius, R_2/a, the mean relative lobe radius, $R_{\rm lobe}/a$, and the masses, $m_{1,2} \sin^3 i$, are given in Table 3. The first quantity, Ω_2, comes mainly from $\Theta_{\rm e}$, as adopted from X-ray eclipse duration, and from the adjusted q. The relative radius is a derived quantity that follows from the adjusted parameters. It varies only slightly among the solutions – less than ± 1 per cent from the mean. More important is the 'lobe status' column, which compares the estimated radius with the lobe radius. As listed, Ω_2 and R_2/a pertain specifically to the case $i = 90°$, $F_2 = 0$. The mass estimates should depend very little on $\Theta_{\rm e}$.

One sees at once that solution 7 stands alone in having a neutron star mass in the low theoretical peak of Timmes et al. (1996). All other estimates correspond to their high-mass peak. Solution 7 utilized the Stickland et al. (1997) ultraviolet RVs based on cross-correlation of 1250- to 1900-Å spectra. The neutron star mass computed by Stickland et al. is 1.39 or 1.33 $M_\odot$, according to two ways of carrying out the solution, and is close to our result from the same data. One must remember, however, that these numbers are $m_1 \sin^3 i$ and that the $\sin^3 i$ factor introduces its own uncertainties (see discussion below). Of course, answers will depend somewhat on the chosen pulse data, but not to a great extent because delay amplitudes vary little among pulse data sets. So, although final numbers will depend on the pulse data and solution method, the Stickland et al. RVs do lead to a neutron star mass sufficiently different from other published values as to have major astrophysical significance. The range of mass estimates for Vela X1 thus remains large, even with advantages (1) to (5) of the Introduction, but at least our unified treatment gives reasonable assurance that the differences are in the data and not in the analyses. The supergiant's mass now shows improved agreement among data sets, with the extremes of our seven results differing from the mean of about 24 $M_\odot$ by only 5 per cent. Supergiant masses as low as 20.5 $M_\odot$ are found in previous results (van Paradijs et al. 1977b). Our solution 1 and 2 $m_2 \sin^3 i$s of 23.3 and 24.3 $M_\odot$ are based on the the van Paradijs et al. RVs.

Most published e and ω estimates are from pulse data, with the es similar on average to those found here ($\approx$0.10). The few RV-based es are typically larger (e.g. 0.223 by Zuiderwijk, van den Heuvel & Hensberge 1974; 0.136 by van Paradijs et al. 1977b), although recently Stickland et al. (1997) found $e = 0.107$. However, our results on ω are quite different from those in the literature, even results from pulse data. Our seven ωs lie in the range 133° to 146° while others' range from about 148° to 177°, except for one KB ω of 121°. The references are KB, BDLZ, Rappaport et al. (1980), Nagase et al. (1984), DBSHNS and van Paradijs et al. (1977b). Published RV-based ωs are 153° (Stickland et al. 1997), 175° (van Paradijs et al. 1977b) and 193° (Zuiderwijk et al. 1974). The only explanation we can offer is our experience that ω is highly correlated with other parameters such that its value depends on the relative weighting of pulse and RV data. One might think that a correctly weighted solution would find ω somewhere between separate pulse and RV solutions, but there is no principle that demands such a result and this certainly is not a precedent (see Van Hamme & Wilson 1990; Eichhorn 1997). Since we have conscientiously applied proper relative pulse and RV weights and the earlier work neglected this point entirely, we think that our results on ω have a good chance of being essentially correct.

A spectacular recent discovery by Kaper et al. (1997) is a bow shock in the interstellar medium, presumably due to collision with GP Vel's stellar wind. The bow shock geometry helps to identify the direction of motion, while position information from the *Hipparcos* satellite provides a rough proper motion, corresponding to about 90 km s^{-1} transverse velocity. The discovery makes GP Vel one of the most interesting cases for examining the runaway star phenomenon. Ordinarily the radial velocity would be the most accurately measured part of the space motion, but here V_γ differs by more than 20 km s^{-1} among RV sets. It would be good to settle the V_γ issue, but all one can do now is point out the inconsistency. Curiously, a majority of RV solution papers fail to list a V_γ, although their solutions almost certainly must have included V_γ.

A claim in several papers (e.g. Nagase 1989; van Kerkwijk et al. 1995) is that information from ellipsoidal variation can be combined with the X-ray eclipse duration to infer the relative radius, R_2/a, and the inclination. While the idea should work for idealized static tides and may work for some real X-ray binaries, it fails demonstrably for Vela X1: GP Vel whose actual ellipsoidal amplitude greatly exceeds that expected in any synchronous or non-synchronous lobe-filling configuration. A likely reason for the large ellipsoidal amplitude is that the tide is not static, but dynamical (Tjemkes et al. 1986; Wilson & Terrell 1994; this paper). Accordingly, any inclination permitted by Table 1 is presently viable and only lower limits are meaningful. Thus we reject published statements to the effect that the Vela X1: GP Vel system has a definitely known inclination (with or without an attached uncertainty), as there is no observational basis for such a claim at present.

More generally – and in opposition to explanations in well-regarded papers, including major reviews – only in exceptional circumstances might one hope to estimate the inclination of *any* HMXB by the traditional means (via $\Theta_{\rm e}$, ellipsoidal variation, etc.), and no other means can realistically be applied at present. The exceptional circumstances would necessarily include high levels of confidence in two items: that the rotation is synchronous and that the optical star accurately fills its limiting lobe. Few, if any, HMXBs are in compliance with these requirements. The point can be illustrated by examining a development in the review by Joss & Rappaport (1984, hereafter JR), also used in the Nagase (1989) review. JR derive an approximate relation between $\sin i$ and several

geometric parameters (their equation 10),

$$\sin i = \left[1 - \beta^2 \left(R_L/a\right)^2\right]^{1/2} / \cos \Theta_e, \tag{4}$$

where R_L is an effective lobe radius, β is the ratio of mean star radius to R_L, and a and Θ_e have their usual meanings. The JR development begins with the well-known formula for eclipse duration by a spherical star and introduces an effective eclipsing radius via an approximation function fitted to equipotential surfaces. JR then state that their formula ' . . . yields inclination angles with typical errors of only $1 - 2°$.' Presumably the errors cited by JR are only the systematic errors of their approximation, but readers could easily misinterpret the remark to mean that inclinations in X-ray binaries can be estimated with realistic errors of 1° to 2°. It appears from comments in the literature (e.g. Timmes et al. 1996, p. 840) that this particular misinterpretation has indeed been made many times. With JR's formula we can quickly see that realistic uncertainties in i (derived from star size and eclipse duration) are so large as to render i completely unknown for typical HMXBs, apart from lower limits. Take a relatively favourable case in which R_L/a is computed without approximation and Θ_e is accurately known, so that the entire error in i comes from uncertainty in β. From (4) the derivative

$$\frac{\mathrm{d}i}{\mathrm{d}\beta} = \frac{-\left(R_L/a\right)^2 \beta}{\left[1 - \beta^2 \left(R_L/a\right)^2\right]^{1/2} \cos i \cos \Theta_e} \tag{5}$$

evaluates in typical HMXB cases to absolute values much above unity – usually 5 rad or greater. Now if β is not known to be unity (exact lobe-filling case, not believed applicable in generic HMXBs), it can only be estimated from ellipsoidal variation and will have an uncertainty of at least a few per cent in any believable situation (remember that β will be correlated with i and F_2, which are fixed parameters in our solutions, and also with q; remember also the erratic light curves of most HMXBs). Therefore the uncertainty in i will be of order ± 0.1 rad ($\pm 6°$) in the most favourable circumstances likely to occur, and usually much larger. Since the above uncertainty estimate ignores errors in Θ_e and any lack of isomorphism between the idealized model and reality, it is clear that the 'standard' geometrical estimation of i gives essentially no useful information for HMXBs. Estimation of $\sin i$ (needed for absolute dimensions and masses) is stronger because of the absence of a $1/\cos i$ factor in $\mathrm{d} \sin i/\mathrm{d}\beta$. Lower limits to i are on a somewhat firmer foundation because they are based on the lobe-filling condition, where β has the definite value of unity. However, even the lower limit is poorly known for Vela X1: GP Vel, as shown by Table 1.

Although the main cause of variable results for Vela X1: GP Vel is the strange behaviour of the optical velocities, we feel that our unified analysis has clarified the situation significantly, with most remaining disagreements due to epoch-to-epoch changes in the data sets. The unified analysis also simplifies the interpretation of multiple kinds of observations because it avoids mutually inconsistent results. The problem of keeping the supergiant within its limiting lobe at periastron has been quantified for seven combinations of RV and pulse observations. Rotation as fast as synchronous is barely possible for some data combinations but slower rotation, such as 0.67 ± 0.04 times the orbital angular rate that follows from line broadening (Zuiderwijk 1995), seems more likely. Further progress toward finding the true orbital parameters and masses would seem to require a breakthrough in radial velocity measurement.

ACKNOWLEDGMENTS

We greatly appreciate discussions with P. E. Boynton and J. E. Deeter about the characteristics of the pulse observations. Our solutions could not have been done without the pulse observations kindly sent by S. Rappaport and by J. E. Deeter. We thank W. Van Hamme for suggesting improvements to the manuscript and also for helping with its preparation.

REFERENCES

Avni Y., 1976, ApJ, 209, 574
Bahcall J. N., 1978, ARA&A, 16, 241
Barone F., Maceroni C., Milano L., Russo G., 1988, A&A, 197, 347
Boynton P. E., Deeter J. E., Lamb F. K., Zylstra G. 1986, ApJ, 307, 545 (BDLZ)
Charles P. A., Mason K. O., White N. E., Culhane J. L., Sanford P. W., 1978, MNRAS, 183, 813
Deeter J. E., Boynton P. E., Shibazaki N., Hayakawa S., Nagase F., Sato N., 1987, AJ, 93, 877 (DBSHNS)
Eichhorn H. K., 1997, A&A, 327, 404
Forman W., Jones C., Tananbaum H., Gursky H., Kellogg E., Giacconi R., 1973, ApJ, 182, L103
Hutchings J. B., 1973, ApJ, 180, 501
Joss P. C., Rappaport S., 1984, ARA&A, 22, 537 (JR)
Kallrath J., Linnell A. P., 1987, ApJ, 313, 346
Kaper L., van Loon J. T., Augusteijn T., Goudfrooij P., Patat F., Waters L. B. F. M., Zijlstra A. A., 1997, ApJ, 475, L37
Limber D. N., 1963, ApJ, 138, 1112
Marquardt D. W., 1963 J. Soc. Indust. Appl. Math., 11, 431
Morbey C. L., 1975, PASP, 87, 689
Nagase F., 1989, PASJ, 41, 1
Nagase F. et al., 1982, ApJ, 263, 814
Nagase F., Hayakawa S., Makino F., Sato N., Makishima K., 1983, PASJ, 35, 47
Nagase F. et al., 1984, ApJ, 280, 259
Ogelman H., Beuermann K. P., Kanbach G., Mayer-Hasselwander H. A., Capozzi D., Fiordilino E., Molteni D., 1977, A&A, 58, 385
Petro L. D., Hiltner W. A., 1974, ApJ, 190, 661
Plavec M. J., 1958, Mem. Soc. R. Liège, 20, 411
Plewa T., 1988, Acta Astron., 38, 415
Pourbaix D., 1998, A&A, submitted
Price W. L., 1976, Comput. J., 20, 367
Rappaport S., Joss P. C., Stothers R., 1980, ApJ, 235, 570
Sato N. et al., 1986, PASJ, 38, 731
Sterne T., 1941, Proc. Nat. Acad. Sci., 27, 168
Stickland D., Lloyd C., Radziun-Woodham A., 1997, MNRAS, 286, L21
Timmes F. X., Woosley S. E., Weaver T. A., 1996, ApJ, 457, 834
Tjemkes S. A., Zuiderwijk E. J., van Paradijs J., 1986, A&A, 154, 77
van Genderen A. M., 1981, A&A, 96, 82
van Kerkwijk M. H., van Paradijs J., Zuiderwijk E. J., Hammerschlag-Hensberge G., Kaper L., Sterken C., 1995, A&A, 303, 483
van der Klis M., Bonnet-Bidaud J. M., 1984, A&A, 135, 155 (KB)
Van Hamme W., Wilson R. E., 1984, A&A, 141, 1
Van Hamme W., Wilson R. E., 1986, AJ, 92, 1168
Van Hamme W., Wilson R. E., 1990, AJ, 100, 1981
Van Hamme W., Wilson R. E., 1994, Mem. Astron. Soc. Ital., 65, 89
Van Hamme W., Wilson R. E., 1997, in Milone E. F., ed., Binary Stars: New Generation Modeling Developments and Results. Univ. Calgary
van Paradijs J., Takens R. J., Zuiderwijk E. J., 1977a, A&A, 57, 221
van Paradijs J., Zuiderwijk E. J., Takens R. J., Hammerschlag-Hensberge G., van den Heuvel E. P. J., de Loore C., 1977b, A&AS, 30, 195
Wallerstein G., 1974, ApJ, 194, 451
Watson M. G., Griffiths R. E., 1977, MNRAS, 178, 513
Wilson R. E., 1979, ApJ, 234, 1054
Wilson R. E., 1994, PASP, 106, 921

Wilson R. E., Devinney E. J., 1972, ApJ, 171, 413
Wilson R. E., Sofia S., 1976, ApJ, 203, 182
Wilson R. E., Terrell D., 1994, in Holt S., Day C. S., eds, The Evolution of X-Ray Binaries. Am. Inst. Phys., New York, p. 483
Wilson R. E., Wilson A. T., 1976, ApJ, 204, 551
Woosley S. E., Weaver T. A., 1995, ApJS, 101, 181
Zuiderwijk E. J., 1995, A&A, 299, 79
Zuiderwijk E. J., van den Heuvel E. P. J., Hensberge G., 1974, A&A, 35, 353

APPENDIX A: PARTIAL DERIVATIVES FOR DIFFERENTIAL CORRECTIONS

The pulse number n (the integer part of pulse phase) is the independent variable and the pulse arrival time t is the dependent variable. The defining equation is

$$t = t_{\rm ref} + S(n - n_{\rm ref})P_{\rm p} + \Delta t - \Delta t_{\rm ref}, \tag{A1}$$

where S is the number of days in a second of time (1/86 400), $P_{\rm p}$ is the pulse period in seconds, and n is an integer assigned to an observed pulse (presumed consecutive in actual pulses, not necessarily in observed pulses). The variable t is in Heliocentric Julian Date (HJD) and Δt is the delay in pulse arrival due to orbit crossing. Positive Δt is the light travel time from the pulsar to a plane normal to the line of sight at the nodal distance ('plane of the sky'), and negative Δt is light travel time from the plane of the sky to the pulsar. Subscript *ref* refers to a designated reference pulse and its time of arrival. All times t, whether subscripted or not, are in the proper time frame of the Solar system barycentre.[1] Implicit parameters that affect t include the system mass ratio ($q = m_2/m_1$), with star 1 the pulse source; the orbital inclination (i) to the plane of the sky, in radians; the relative orbital semi-major axis ($a = a_1 + a_2$), here in solar radii; the orbital eccentricity, e; the argument of periastron, ω, in radians; the orbital period, $P_{\rm orb}$, here in mean solar days; and the orbital time reference, t_0. The implicit parameters enter through the delay terms, which depend on location within the orbit. Parameters $P_{\rm p}$ and $t_{\rm ref}$ enter both explicitly through the first two terms of (A1) and implicitly via the computation of time and thus of orbital position and delay. One uses the pulse ephemeris to obtain time, then the orbital ephemeris to obtain orbital phase, and finally the orbital phase to compute delay. Thus recognize the first two terms of (A1) as time, $t_{\rm p}$, kept by the pulsar clock (also in HJD),

$$t_{\rm p} = t_{\rm ref} + S(n - n_{\rm ref})P_{\rm p}, \tag{A2}$$

which then is coupled to the orbital phase, ϕ, by

$$\phi = \phi_0 + \frac{(t_{\rm p} - t_0)}{P_{\rm orb}}. \tag{A3}$$

Here t_0 and ϕ_0 are respectively the orbital reference epoch (time of superior conjunction of star 1) and the phase assigned to that epoch. Often ϕ_0 will simply be zero, but in general we allow the phase to include a constant offset. The computed times depend on the nine parameters $t_{\rm ref}$, q, i, a, e, ω, t_0, $P_{\rm p}$ and $P_{\rm orb}$. Partial derivatives, $\partial t/\partial p$, of arrival time with respect to the parameters are needed if one is to fit pulse observations by the method of differential corrections. First, the explicit form of the delays must be specified:

$$\Delta t = \frac{S{\rm R}_\odot a D q \sin i}{c(1+q)}\cos(2\pi\phi_{\rm g}), \tag{A4}$$

[1]We neglect relativistic effects, which are very small in the context of typical X-ray binaries.

where $\rm R_\odot$ is the radius of the Sun in kilometers, D is the instantaneous separation of the two stars (unit = relative semi-major axis), $\phi_{\rm g}$ is the angle in the orbit plane measured from conjunction in the direction of motion (we call $\phi_{\rm g}$ the 'geometrical phase', with unit that of conventional phase, 2π radians), and c is the speed of light in kilometers per second. Formally,

$$\phi_{\rm g} = \frac{v + \omega}{2\pi} - 0.25, \tag{A5}$$

where v is the true anomaly (angle from periastron to star in the orbit plane). The $\Delta t_{\rm ref}$ term is the same as Δt, except for *ref* subscripts ($D_{\rm ref}$ and $\phi_{\rm g_{ref}}$). Next a relation between orbital phase and orbital angle, $\phi_{\rm g}$, is required. The mean anomaly, M, is the difference between a given phase and periastron phase, $\phi_{\rm per}$,

$$M = 2\pi(\phi - \phi_{\rm per}) \tag{A6}$$

with

$$\phi_{\rm per} = \omega/(2\pi) + \phi_0 + 0.75, \tag{A7}$$

where the 0.75 term accounts for ω being measured from the ascending node (270° from conjunction). So

$$M = 2\pi(\phi - \phi_0) - \omega - 1.5\pi. \tag{A8}$$

However, ϕ includes ϕ_0 (cf. A3), so M does not depend on ϕ_0 but does depend on t_0.

$$M = 2\pi\frac{(t_{\rm p} - t_0)}{P_{\rm orb}} - \omega - 1.5\pi. \tag{A9}$$

The eccentric anomaly, E, also occurs below. In the interest of compactness, we define expressions that occur repeatedly. They are

$$\Delta x = D\cos(2\pi\phi_{\rm g}) - D_{\rm ref}\cos(2\pi\phi_{\rm g_{ref}}), \tag{A10}$$

$$A = S{\rm R}_\odot/c, \tag{A11}$$

$$B = \sqrt{\frac{1+e}{1-e}}, \tag{A12}$$

$$Q = \frac{q}{1+q}, \tag{A13}$$

$$\frac{{\rm d}M}{{\rm d}\phi} = 2\pi, \tag{A14}$$

$$\frac{{\rm d}\phi_{\rm g}}{{\rm d}v} = \frac{1}{2\pi}, \tag{A15}$$

$$\frac{\partial D}{\partial v} = \frac{e(1-e^2)\sin v}{(1+e\cos v)^2}, \tag{A16}$$

$$\frac{{\rm d}v}{{\rm d}M} = B\frac{\cos^2(0.5v)}{\cos^2(0.5E)(1-e\cos E)}, \tag{A17}$$

$$\frac{{\rm d}D}{{\rm d}M} = \frac{\partial D}{\partial v}\frac{{\rm d}v}{{\rm d}M}, \tag{A18}$$

$$\frac{{\rm d}\phi_{\rm g}}{{\rm d}M} = \frac{{\rm d}\phi_{\rm g}}{{\rm d}v}\frac{{\rm d}v}{{\rm d}M}. \tag{A19}$$

The required partial derivatives are

$$\frac{\partial t}{\partial q} = \frac{Aa\sin i}{(1+q)^2}\Delta x, \tag{A20}$$

$$\frac{\partial t}{\partial i} = AaQ\cos i\Delta x, \tag{A21}$$

$$\frac{\partial t}{\partial a} = AQ\sin i\Delta x, \tag{A22}$$

$$\frac{\partial t}{\partial t_{\rm ref}} = 1 + AaQ\sin i \begin{bmatrix} \cos(2\pi\phi_{\rm g})\frac{{\rm d}D}{{\rm d}t_{\rm ref}} \\ -\cos(2\pi\phi_{g_{\rm ref}})\frac{{\rm d}D_{\rm ref}}{{\rm d}t_{\rm ref}} \\ -2\pi D\sin(2\pi\phi_{\rm g})\frac{{\rm d}\phi_{\rm g}}{{\rm d}t_{\rm ref}} \\ +2\pi D_{\rm ref}\sin(2\pi\phi_{g_{\rm ref}})\frac{{\rm d}\phi_{g_{\rm ref}}}{{\rm d}t_{\rm ref}} \end{bmatrix}, \tag{A23}$$

with

$$\frac{{\rm d}D}{{\rm d}t_{\rm ref}} = \frac{{\rm d}D}{{\rm d}M}\frac{{\rm d}M}{{\rm d}t_{\rm p}}\frac{{\rm d}t_{\rm p}}{{\rm d}t_{\rm ref}}, \tag{A24}$$

$$\frac{{\rm d}\phi_{\rm g}}{{\rm d}t_{\rm ref}} = \frac{{\rm d}\phi_{\rm g}}{{\rm d}M}\frac{{\rm d}M}{{\rm d}t_{\rm p}}\frac{{\rm d}t_{\rm p}}{{\rm d}t_{\rm ref}}, \tag{A25}$$

$$\frac{{\rm d}M}{{\rm d}t_{\rm p}} = \frac{2\pi}{P_{\rm orb}}, \tag{A26}$$

$$\frac{{\rm d}t_{\rm p}}{{\rm d}t_{\rm ref}} = 1. \tag{A27}$$

$$\frac{\partial t}{\partial e} = AaQ\sin i \begin{bmatrix} \cos(2\pi\phi_{\rm g})\frac{{\rm d}D}{{\rm d}e} \\ -\cos(2\pi\phi_{g_{\rm ref}})\frac{{\rm d}D_{\rm ref}}{{\rm d}e} \\ -2\pi D\sin(2\pi\phi_{\rm g})\frac{{\rm d}\phi_{\rm g}}{{\rm d}e} \\ +2\pi D_{\rm ref}\sin(2\pi\phi_{g_{\rm ref}})\frac{{\rm d}\phi_{g_{\rm ref}}}{{\rm d}e} \end{bmatrix}, \tag{A28}$$

with

$$\frac{{\rm d}D}{{\rm d}e} = \frac{\partial D}{\partial v}\frac{{\rm d}v}{{\rm d}e} + \frac{\partial D}{\partial e}, \tag{A29}$$

$$\frac{\partial D}{\partial e} = -\frac{(1+e^2)\cos v + 2e}{(1+e\cos v)^2}, \tag{A30}$$

$$\frac{{\rm d}\phi_{\rm g}}{{\rm d}e} = \frac{{\rm d}\phi_{\rm g}}{{\rm d}v}\frac{{\rm d}v}{{\rm d}e}, \tag{A31}$$

$$\frac{{\rm d}v}{{\rm d}e} = \cos(0.5v)\left[\frac{B\sin E\cos(0.5v)}{(1-e\cos E)\cos^2(0.5E)} + \frac{2\sin(0.5v)}{1-e^2}\right], \tag{A32}$$

$$\frac{\partial t}{\partial \omega} = AaQ\sin i \begin{bmatrix} \cos(2\pi\phi_{\rm g})\frac{{\rm d}D}{{\rm d}\omega} \\ -\cos(2\pi\phi_{g_{\rm ref}})\frac{{\rm d}D_{\rm ref}}{{\rm d}\omega} \\ -2\pi D\sin(2\pi\phi_{\rm g})\frac{{\rm d}\phi_{\rm g}}{{\rm d}\omega} \\ +2\pi D_{\rm ref}\sin(2\pi\phi_{g_{\rm ref}})\frac{{\rm d}\phi_{g_{\rm ref}}}{{\rm d}\omega} \end{bmatrix}, \tag{A33}$$

with

$$\frac{{\rm d}D}{{\rm d}\omega} = \frac{\partial D}{\partial v}\frac{{\rm d}v}{{\rm d}\omega}, \tag{A34}$$

$$\frac{{\rm d}\phi_{\rm g}}{{\rm d}\omega} = \frac{1}{2\pi}\left(\frac{{\rm d}v}{{\rm d}\omega} + 1\right), \tag{A35}$$

$$\frac{{\rm d}v}{{\rm d}\omega} = \frac{B}{(1-e\cos E)}\frac{\cos^2(0.5v)}{\cos^2(0.5E)}\frac{{\rm d}M}{{\rm d}\omega}, \tag{A36}$$

$$\frac{{\rm d}M}{{\rm d}\omega} = -1. \tag{A37}$$

$$\frac{\partial t}{\partial t_0} = AaQ\sin i \begin{bmatrix} \cos(2\pi\phi_{\rm g})\frac{{\rm d}D}{{\rm d}t_0} \\ -\cos(2\pi\phi_{g_{\rm ref}})\frac{{\rm d}D_{\rm ref}}{{\rm d}t_0} \\ -2\pi D\sin(2\pi\phi_{\rm g})\frac{{\rm d}\phi_{\rm g}}{{\rm d}t_0} \\ +2\pi D_{\rm ref}\sin(2\pi\phi_{g_{\rm ref}})\frac{{\rm d}\phi_{g_{\rm ref}}}{{\rm d}t_0} \end{bmatrix}, \tag{A38}$$

with

$$\frac{{\rm d}D}{{\rm d}t_0} = \frac{{\rm d}D}{{\rm d}M}\frac{{\rm d}M}{{\rm d}t_0}, \tag{A39}$$

$$\frac{{\rm d}\phi_{\rm g}}{{\rm d}t_0} = \frac{{\rm d}\phi_{\rm g}}{{\rm d}M}\frac{{\rm d}M}{{\rm d}t_0}, \tag{A40}$$

$$\frac{{\rm d}M}{{\rm d}t_0} = -\frac{2\pi}{P_{\rm orb}}. \tag{A41}$$

$$\frac{\partial t}{\partial P_{\rm p}} = S(n-n_{\rm ref}) + AaQ\sin i \begin{bmatrix} \cos(2\pi\phi_{\rm g})\frac{{\rm d}D}{{\rm d}P_{\rm p}} \\ -2\pi D\sin(2\pi\phi_{\rm g})\frac{{\rm d}\phi_{\rm g}}{{\rm d}P_{\rm p}} \end{bmatrix} \tag{A42}$$

(Note: the terms subscripted 'ref' do not appear in A42 because ${\rm d}t_{\rm p_{ref}}/{\rm d}P_{\rm p}$ (see below) is zero.)

with

$$\frac{{\rm d}D}{{\rm d}P_{\rm p}} = \frac{{\rm d}D}{{\rm d}M}\frac{{\rm d}M}{{\rm d}\phi}\frac{{\rm d}\phi}{{\rm d}t_{\rm p}}\frac{{\rm d}t_{\rm p}}{{\rm d}P_{\rm p}}, \tag{A43}$$

$$\frac{{\rm d}\phi_{\rm g}}{{\rm d}P_{\rm p}} = \frac{{\rm d}\phi_{\rm g}}{{\rm d}M}\frac{{\rm d}M}{{\rm d}\phi}\frac{{\rm d}\phi}{{\rm d}t_{\rm p}}\frac{{\rm d}t_{\rm p}}{{\rm d}P_{\rm p}}, \tag{A44}$$

$$\frac{{\rm d}\phi}{{\rm d}t_{\rm p}} = \frac{1}{P_{\rm orb}}, \tag{A45}$$

$$\frac{{\rm d}t_{\rm p}}{{\rm d}P_{\rm p}} = S(n-n_{\rm ref}). \tag{A46}$$

$$\frac{\partial t}{\partial P_{\rm orb}} = AaQ\sin i \begin{bmatrix} \cos(2\pi\phi_{\rm g})\frac{{\rm d}D}{{\rm d}P_{\rm orb}} \\ -\cos(2\pi\phi_{g_{\rm ref}})\frac{{\rm d}D_{\rm ref}}{{\rm d}P_{\rm orb}} \\ -2\pi D\sin(2\pi\phi_{\rm g})\frac{{\rm d}\phi_{\rm g}}{{\rm d}P_{\rm orb}} \\ +2\pi D_{\rm ref}\sin(2\pi\phi_{g_{\rm ref}})\frac{{\rm d}\phi_{g_{\rm ref}}}{{\rm d}P_{\rm orb}} \end{bmatrix}, \tag{A47}$$

with

$$\frac{{\rm d}D}{{\rm d}P_{\rm orb}} = \frac{{\rm d}D}{{\rm d}M}\frac{{\rm d}M}{{\rm d}\phi}\frac{{\rm d}\phi}{{\rm d}P_{\rm orb}}, \tag{A48}$$

$$\frac{{\rm d}\phi_{\rm g}}{{\rm d}P_{\rm orb}} = \frac{{\rm d}\phi_{\rm g}}{{\rm d}M}\frac{{\rm d}M}{{\rm d}\phi}\frac{{\rm d}\phi}{{\rm d}P_{\rm orb}}, \tag{A49}$$

$$\frac{{\rm d}\phi}{{\rm d}P_{\rm orb}} = -\frac{t_{\rm p}-t_0}{P_{\rm orb}^2}. \tag{A50}$$

This paper has been typeset from a TEX/LATEX file prepared by the author.